

## Dynamic Mechanical Properties of Cross-Linked Rubbers.

### VII. Butyl Rubber Networks

James F. Sanders and John D. Ferry\*<sup>1</sup>

Department of Chemistry, University of Wisconsin, Madison, Wisconsin 53706.  
Received March 27, 1974

**ABSTRACT:** The linear viscoelastic properties of seven samples of butyl rubber, cross-linked by sulfur to different extents, have been studied in shear by dynamic and creep measurements. The frequency and temperature ranges were 0.1 to 600 Hz and  $-25$  to  $55^\circ$ , and creep times extended to  $10^5$  sec. The creep data were converted to the corresponding dynamic viscoelastic functions at very low frequencies. All data were reduced to  $T_0 = 298^\circ\text{K}$  by shift factors calculated from the equation  $\log a_T = -9.03 (T - T_0)/(201.6 + T - T_0)$ . All the viscoelastic functions displayed two principal regions of frequency dependence. The behavior in the transition zone (higher frequencies) was closely similar for all degrees of cross-linking and for the nearly chemically identical uncross-linked polymer polyisobutylene. There was a slight shift to longer times with increasing cross-linking. The plateau compliance  $J_{eN}$  was obtained by suitable integrations of the loss compliance  $J''$  or the retardation spectrum  $L$ . Its reciprocal,  $G_{eN}$ , increased somewhat with the degree of cross-linking; it was extrapolated to  $2.9 \times 10^6$  dyn/cm<sup>2</sup> to zero cross-linking, again in reasonable agreement with that of polyisobutylene and corresponding to an average molecular weight between entanglements of 8500. From measurements at low frequencies or long times, the contributions of slow mechanisms to  $L$  are found to increase rapidly with diminishing cross-linking as found for other rubberlike polymers. Data for several lightly cross-linked polymers with comparable ratios of cross-link spacing to entanglement spacing were compared with the time scale reduced to corresponding states of molecular mobility as gauged by the monomeric friction coefficient. The broad secondary maximum in  $L$  occurs at approximately the same point on the reduced time scale (within a decade), indicating that the long-range motions responsible for the slow mechanisms are similar in all the polymers.

In previous papers of this series, viscoelastic properties of various cross-linked rubbers were described, including natural rubber,<sup>2</sup> 1,4-polybutadiene,<sup>3</sup> styrene-butadiene rubber,<sup>4</sup> and poly(dimethylsiloxane).<sup>5</sup> Particular attention was devoted to relaxation times which are observed in networks with low degrees of cross-linking and have been attributed primarily to motion of untrapped entanglements.<sup>5,6</sup> In the present study, similar data are reported for butyl rubber. This polymer is of particular interest because it has a far lower molecular mobility than any of those previously investigated;<sup>7</sup> this behavior has been attributed to differences in local motions, associated with the strong steric hindrance of the methyl groups.<sup>8</sup>

#### Experimental Section

**Materials.** The samples of cross-linked butyl rubber were generously provided by Drs. P. Thirion and R. Chasset of the Institut Français du Caoutchouc, Paris. Their unvulcanized precursor was Polysar 600; its number-average molecular weight from osmotic pressure measurements<sup>9</sup> in toluene was  $1.66 \times 10^5$ . The composition was 100 parts rubber, 0.5 stearic acid, 3 zinc oxide, 1.5 sulfur, 0.6 2,2'-dibenzothiazyl disulfide, and 2.8 tellurium diethyldithiocarbamate. Two series were vulcanized at 140 and 150°, respectively, for times ranging from 3 to 40 min. The density of all samples was  $0.957 \pm 0.0005$  g/cm<sup>3</sup>. Disk-shaped samples, 1.75 cm in diameter, were cut for viscoelastic measurements.

**Methods.** The Fitzgerald transducer<sup>10</sup> was used for measurements of the storage ( $J'$ ) and loss ( $J''$ ) components of the complex dynamic shear compliance in the range from 45 to 600 Hz, over the temperature range from  $-25$  to  $50^\circ$ . The Plazek torsion pendulum<sup>11</sup> was used for dynamic measurements in the range from 0.1 to 1 Hz at temperatures from  $-2$  to  $55^\circ$  and for creep measurements over time periods up to  $10^5$  sec. Modifications in the original apparatus have been reported elsewhere.<sup>2b,5,12</sup> Air was excluded by a continuous flow of nitrogen. Creep measurements at shorter times than previously achieved ( $\geq 5$  sec) were accomplished by use of a Sanborn recorder.

#### Results

Both creep and dynamic data were reduced to a temperature of  $25^\circ$  by shift factors  $a_T$  calculated from the WLF equation<sup>13</sup> with parameters chosen for the best fit to the transition zone data obtained with the Fitzgerald apparatus:  $c_1 = 9.03$  and  $c_2 = 201.6$ . These agree rather well with

the corresponding values for the almost chemically identical polymer polyisobutylene, the temperature dependence data of which can be fitted<sup>14</sup> with  $c_1 = 8.61$  and  $c_2 = 200.4$ . The thermal expansion coefficient was taken as  $5.8 \times 10^{-4}$  deg<sup>-1</sup>, the value of polyisobutylene.

In Figure 1, the reduced creep compliance  $J_p(t) = (T/\rho T_0 \rho_0)J(t)$ , where  $J(t)$  is the measured compliance,  $T$  and  $\rho$  the temperature of measurement and the corresponding density, and  $T_0$  and  $\rho_0$  the reference temperature and density, is plotted logarithmically against  $t/a_T$ , with  $t$  in seconds. In three cases, very small vertical adjustments ( $\Delta \log J_p(t) \leq 0.008$ ) have been made to give exact coincidence of data at different temperatures; the deviations were attributed to slight errors in measurements of sample thickness, and the values nearest room temperature were taken as correct.<sup>5</sup> As usual, increasing cross-linking diminishes both the magnitude of the compliance and its time dependence. Numerical data are given elsewhere.<sup>15</sup>

The equilibrium compliance  $J_e$  was estimated by extrapolation to infinite time, fitting the creep data to an empirical equation adapted from an equation of Thirion and Chasset<sup>16</sup>

$$J(t) = J_e / [1 + (t/t_m)^{-m}] \quad (1)$$

both by a graphical method previously described<sup>2b</sup> and by a computer program which provided a nonlinear least-squares regression analysis;<sup>17</sup> the two methods agreed well and the extrapolated values are listed in Table I. Values of  $m$  and  $m \log t_m$  from the regression analysis are also given. It is puzzling that the exponent  $m$  changes with cross-linking in the opposite direction to that usually observed,<sup>2-4,16</sup> and the magnitudes of the parameters imply that exceedingly long times would be required to approach within 1% of equilibrium. Hence the values of  $J_e$ , especially for the lighter degrees of cross-linking, are somewhat doubtful. However, reasonable agreement was obtained with the equilibrium compliance estimated by the time scale shift procedure of Plazek,<sup>18</sup> which could be applied to only three of the samples (assuming the value from eq 1 for sample 15-150 to be correct; it cannot be much in error because of

**Table I**  
**Characterization and Viscoelastic Data**

| Sample code <sup>a</sup> | $-\log J_e, \text{cm}^2/\text{dyn}$ |                      | $m$   | $m \log t_m,$<br>$t_m$ in sec | $J_{eN} \times 10^7$ |          |
|--------------------------|-------------------------------------|----------------------|-------|-------------------------------|----------------------|----------|
|                          | Eq 1                                | P <sup>b</sup>       |       |                               | Method 1             | Method 2 |
| 3-140                    | 5.77                                |                      | 0.158 | 0.516                         | 3.25                 | 3.34     |
| 5-140                    | 5.85                                |                      | 0.128 | 0.422                         | 3.36                 |          |
| 10-140                   | 6.26                                | 6.33                 | 0.050 | -0.125                        | 2.94                 |          |
| 7-150                    | 6.42 <sub>5</sub>                   | 6.41                 | 0.085 | -0.562                        | 2.82                 | 2.79     |
| 10-150                   | 6.52 <sub>5</sub>                   | 6.53 <sub>7</sub>    | 0.057 | -0.680                        | 2.36                 |          |
| 15-150                   | 6.57 <sub>5</sub>                   | (6.57 <sub>5</sub> ) | 0.054 | -0.782                        | 2.24                 |          |
| 40-150                   | 6.60 <sub>2</sub>                   |                      | 0.050 | -0.865                        | 2.15                 | 1.95     |

<sup>a</sup> First number denotes vulcanization time in min, second number vulcanization temperature. <sup>b</sup> Estimated from scale shift method of Plazek.<sup>18</sup>

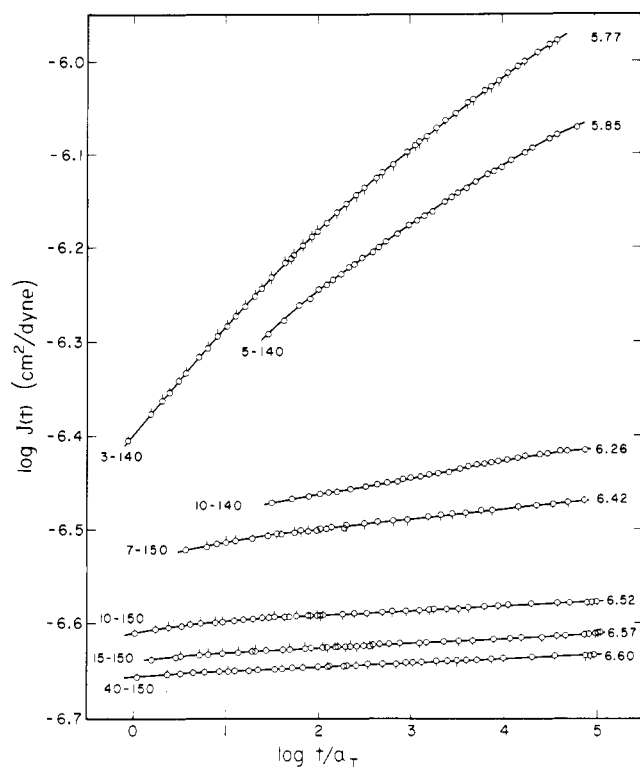


**Figure 1.** Creep compliance plotted logarithmically against time reduced to 25°. Numbers at left denote sample code, at right  $-\log J_e$ . Circles without pips, measured near room temperature (22.3 to 25.8°); with pips, at a lower temperature (-1.3 to -5.0°). Some points omitted to avoid confusion.

the very slight time dependence of  $J(t)$ . The extrapolated values of  $J_e$  are shown in Figure 1 as a measure of the degree of cross-linking.

The torsion pendulum data, taken at up to seven different temperatures with usually a room temperature check run at the end, superposed well when reduced and because of somewhat less precision than for creep, no need for vertical adjustments was detected. The Fitzgerald transducer data, taken at up to 15 different temperatures with check runs, superposed well when reduced. Comparison of the reduced torsion pendulum and transducer data where they overlapped near  $\log a_T = 2$  showed agreement of the loss tangent  $\tan \delta = J''/J'$ , but some divergence in  $J'$  and  $J''$ , attributed as usual to uncertainty in measurement of sample thickness in the transducer.<sup>3</sup> The transducer data were adjusted where necessary (0.04 log units or less) to match the torsion pendulum data.

In Figures 2 and 3, the reduced dynamic data for  $J'$  and  $J''$  are plotted logarithmically against  $\omega a_T$ , where  $\omega$  is ra-

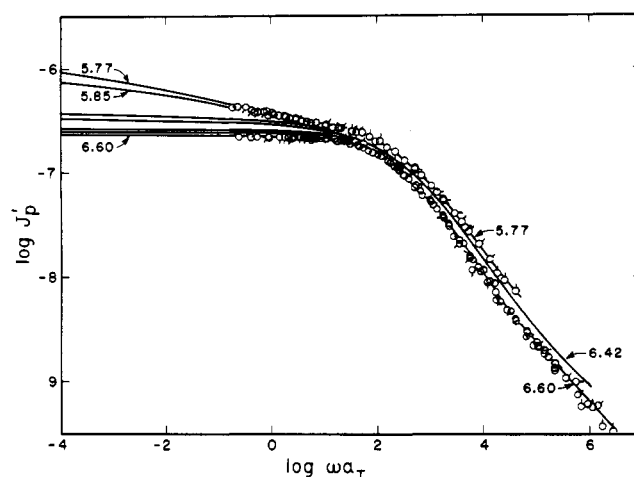


**Figure 2.** Storage compliance, reduced to 25°, plotted logarithmically against frequency. Samples identified by values of  $-\log J_e$ . Curves for  $\log \omega a_T < -1$  calculated from creep data of Figure 1. Pips denote individual temperatures. Points omitted from intermediate curves to avoid confusion.

dian frequency, and combined with equivalent low-frequency curves calculated from the data of Figure 1 by customary approximation formulas.<sup>15,19</sup> The loss tangent is plotted in Figure 4. As observed for the polymers studied previously, the transition zone is almost unaffected by the extent of cross-linking, but there is an additional relaxation mechanism at low frequencies whose prominence increases with diminishing cross-link density.

## Discussion

**Retardation and Relaxation Spectra.** The retardation spectrum  $L$  was calculated from the data of Figures 1, 2, and 3 by customary approximation formulas and is plotted logarithmically in Figure 5. This shows again the presence of mechanisms with very long retardation times, whose contributions to compliance increase rapidly with diminishing cross-link density. The figure shows no indication of the vanishing of  $L$  at long times, necessary for a finite value of  $J_e$ , but the parameters of Table I imply that this occurs well beyond the experimental time scale; the form of eq 1 ensures that the integral of  $Ld \ln \tau$  converges.<sup>2b</sup> The retardation spectrum of polyisobutylene, essentially equivalent to uncross-linked butyl rubber, from measurements 20 years earlier,<sup>20,21</sup> is included for comparison. In the transition zone, the uncross-linked polymer and all the cross-linked samples are very similar; the small shift to longer times with increasing cross-linking is probably due to the chemical modification by combined sulfur.<sup>2a,3</sup>

Relaxation spectra  $H$  were also calculated by converting  $J'$  and  $J''$  to the components of the complex modulus  $G'$  and  $G''$ , and applying customary approximation formulas.

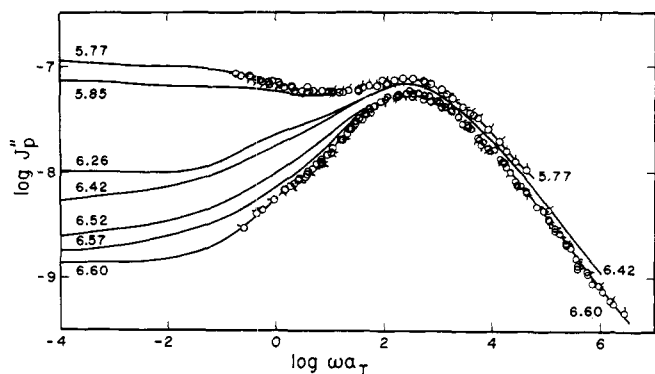


Figure 3. Loss compliance, reduced and plotted as in Figure 2.

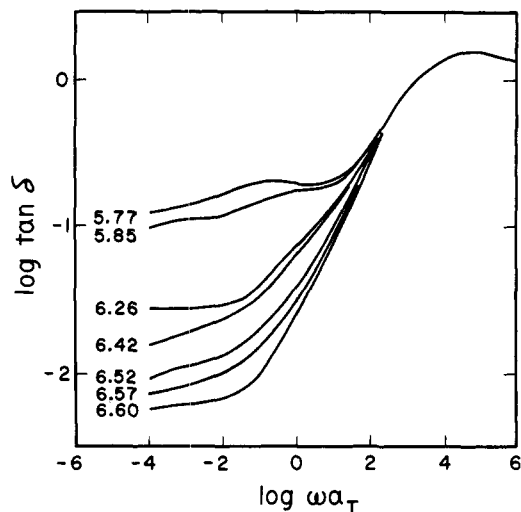


Figure 4. Loss tangent plotted logarithmically against frequency reduced to 25°. Samples identified by values of  $-\log J_e$ .

The results (not shown) almost coincided in the transition zone from  $\log \tau = -4$  to  $-2$  with a slope close to  $-1/2$  on a logarithmic plot, and from the magnitude of  $H$  in this region the parameter  $a^2\zeta_0/M_0^2$  was calculated from the Rouse-Mooney theory as a gauge of molecular mobility for comparison with other polymers.<sup>4</sup> Here  $a^2$  is the mean square end-to-end distance per monomer unit,  $\zeta_0$  the monomeric friction coefficient, and  $M_0$  the monomer molecular weight;  $\log a^2\zeta_0/M_0^2 = -22.12$  at 25°.

**Evaluation of Plateau Compliance.** The plateau compliance  $J_{eN}$  which includes all contributions from the transition zone but none from the secondary mechanisms with long retardation times, corresponding qualitatively to the magnitude of  $J'$  at  $\log \omega a_T = 0.2$  in Figure 2, can be evaluated in two ways. (1) A linear plot of  $L$  is resolved, with some arbitrariness, to separate the contribution of the transition zone; the remainder is integrated graphically to obtain  $\int_{-\infty}^{\ln t_1} L d \ln \tau$  to the longest time of measurement,  $t_1$ , denoted  $J_{e2}$ ; the integral from  $t_1$  to  $\infty$ , denoted  $J_{e1}$ , is obtained analytically from the parameters of eq 1; and finally,  $J_{eN} = J_e - J_{e1} - J_{e2}$ .<sup>2-5</sup> (It may be mentioned that any error in extrapolating  $J_e$  will be reproduced in  $J_{e1}$  and hence should not affect the calculation of  $J_{eN}$ .) (2) A linear plot of  $J''$  is resolved, with some arbitrariness, to separate the contribution of the transition zone, and this contribution is graphically integrated to obtain  $J_{eN} = (2/\pi) \int_a^\infty J'' d \ln \omega$ ;  $a$  is the logarithm of the lowest frequency at which the transition zone makes a significant contribution.<sup>22</sup> Method (2) is applicable only if data are available throughout the transition zone, as is the case here for three of the

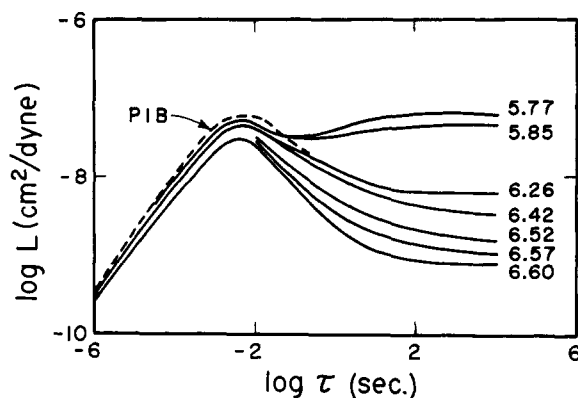


Figure 5. Retardation spectra plotted logarithmically, reduced to 25°. Solid curves, butyl rubber samples identified by values of  $-\log J_e$ ; dashed curve, polyisobutylene.<sup>20</sup>

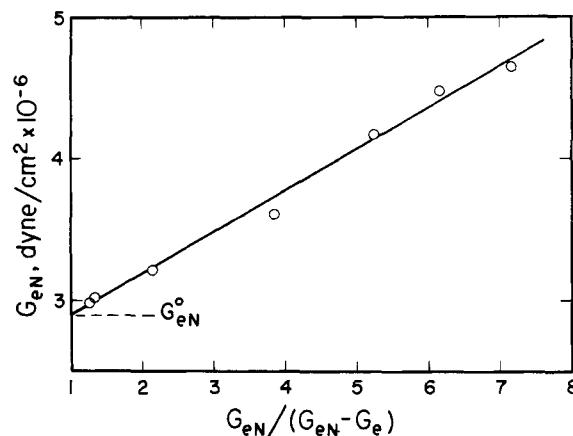


Figure 6. Plot of  $G_{eN}$  against  $G_{eN}/(G_{eN} - G_e)$ , with extrapolation to  $G_{eN}^0$ .

samples. Calculations from both methods are given in Table I and agree well.

The magnitude of  $G_{eN} = 1/J_{eN}$  reflects the density of network strands terminated by both entanglements and cross-links, and it increases with the degree of cross-linking. Extrapolated to zero cross-linking, it should become  $G_{eN}^0$ , the plateau modulus of the uncross-linked polymer which reflects entanglements alone. A convenient linear extrapolation is shown in Figure 6, where  $G_{eN}$  is plotted against  $G_{eN}/(G_{eN} - G_e)$ . Unity on the abscissa scale corresponds to zero cross-linking; the extrapolated ordinate is  $2.9 \times 10^6$  dyn/cm<sup>2</sup>, a value which has been used<sup>15</sup> to estimate the entanglement spacing in butyl rubber as 8500. As expected, it is close to the corresponding value for polyisobutylene,  $2.5 \times 10^6$  dyn/cm<sup>2</sup>, derived from integration of the loss compliance.<sup>22</sup> (Plots similar to Figure 6 with data for other polymers<sup>2-4</sup> are also roughly linear but with different slopes. No theoretical significance is attached to this relation.)

If the contributions of entanglements and cross-links to the plateau modulus were simply additive, we should expect  $G_{eN} = G_{eN}^0 + G_x$  and  $G_e = G_{eN}^0 T_e + G_x$ , where  $G_x$  is the contribution from cross-links and  $T_e$  is the proportion of entanglements which are trapped and contribute to the modulus at equilibrium. Actually, unless the number of cross-linked points per molecule is quite high, the presence of sol fraction and loose ends necessitates some much more complicated relations, as derived by Langley.<sup>6,23</sup> Nevertheless, for the higher degrees of cross-linking, simple additivity is not too bad; for sample 40-150, it leads to  $G_x = 1.75 \times$

**Table II**  
Polymers in Corresponding States

| Polymer                      | Ref      | Sample code        | $\log a^2 \zeta_0 / M_0^2$ | $M_c / M_e$ | $2M_c^2 / M_e \bar{M}_n$ |
|------------------------------|----------|--------------------|----------------------------|-------------|--------------------------|
| Butyl rubber (BR)            | Figure 5 | 3-140              | -22.1                      | 4.7         | 2.3                      |
| Natural rubber (NR)          | 2        | B <sub>1</sub> -20 | -24.4                      | 6.7         | 1.2                      |
| Styrene-butadiene (SBR)      | 4        | 93-20              | -24.0                      | 5.0         | 1.5                      |
| Polybutadiene (c-t PB)       | 3        | 734                | -24.7                      | 4.2         | 0.4                      |
| Polydimethyl siloxane (PDMS) | 5        | A-4                | -25.7                      | 3.0         | 0.3                      |

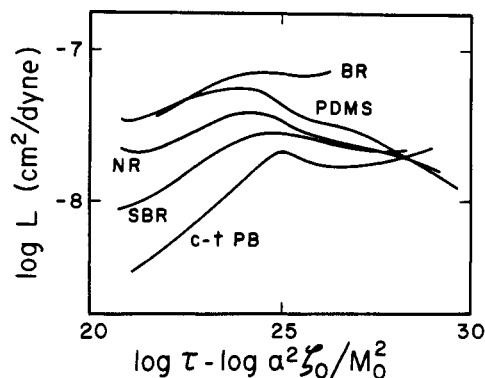


**Figure 7.** Retardation spectra of five rubbery polymers, identified as in Table II, in the region of slow mechanisms, with time scale reduced to correspond to coincidence of transition zones.

$10^6$  and  $T_e = 0.78$ , whereas the Langley theory for an initial most probable distribution and 12 cross-link points per molecule (number-average, corresponding to the given value of  $G_x$ ) predicts  $T_e = 0.74$ .

**Location of Slow Retardation Mechanisms on the Time Scale.** The position of the very broad secondary maximum in  $L$  at long times at  $25^\circ$  (seen only in the uppermost curve in Figure 5) depends of course on chemical structure; for butyl rubber it is near  $10^2$  sec, for poly(dimethyl siloxane)<sup>5</sup> it is near  $10^{-2}$  sec. It is of interest to examine whether these differences reflect primarily the local molecular mobility as gauged by the monomeric friction coefficient  $\zeta_0$ ; if the nature of the exceedingly slow motions is similar for all polymers, the long retardation times should be proportional to  $\zeta_0$  as are the much shorter times which describe behavior in the transition zone. Actually, in comparing different polymers, it is more convenient to characterize the location of the transition zone by the parameter  $a^2 \zeta_0 / M_0^2$  cited above; the logarithm of this quantity at  $25^\circ$  is given in Table II for several polymers. Plots of  $\log L$  against  $\log \tau - \log a^2 \zeta_0 / M_0^2$  place different polymers in corresponding states with respect to the transition zone.

In comparing such data, polymers with corresponding degrees of cross-linking should be chosen. Possible indices of correspondence might be  $M_c / M_e$ , a measure of the average number of entanglements per strand of the cross-linked network, or per unbranched loose end, or  $2M_c^2 / M_e \bar{M}_n$ , a measure of the number of entanglements on loose ends. (Here,  $M_c$  is the average molecular weight between cross-links, estimated very roughly as  $\rho RT J_e$  without correction for trapped entanglements and loose ends.) These ratios are listed in Table II for the lightly cross-linked samples which have been chosen for comparison; the former, at least, is approximately the same for all the polymers. The plot against reduced time is shown in Figure 7. The transition zone would lie far to the left. The maxima associated with the slow mechanisms agree in position within about a

decade; in particular, BR and PDMS nearly coincide, though separated by 4 decades before reduction. Thus, qualitatively, the very slow motions appear to be of similar character in all the polymers.

The slow relaxation processes studied here have been attributed primarily to rearrangement of untrapped entanglements on branched dangling structures in polymers with low degrees of cross-linking.<sup>5,6</sup> Recent experiments of Tschoegl and associates<sup>24</sup> with block copolymers indicate that trapped entanglements can also be associated with slow relaxation processes. Because the structure and network topology of vulcanizates such as studied here cannot be easily controlled and characterized, new experiments have been undertaken with networks containing loose repeating molecules which participate in untrapped entanglements only.<sup>25</sup> These will be reported in more detail subsequently.<sup>26</sup>

**Acknowledgments.** This work was supported in part by grants from the National Science Foundation and the Army Research Office-Durham.

## References and Notes

- (1) Author to whom correspondence should be addressed.
- (2) (a) J. D. Ferry, R. G. Mancke, E. Maekawa, Y. Oyanagi, and R. A. Dickie, *J. Phys. Chem.*, **68**, 3414 (1964); (b) R. A. Dickie and J. D. Ferry, *ibid.*, **70**, 2594 (1966).
- (3) E. Maekawa, R. G. Mancke, and J. D. Ferry, *J. Phys. Chem.*, **69**, 2811 (1965).
- (4) R. G. Mancke and J. D. Ferry, *Trans. Soc. Rheol.*, **12**, 335 (1968).
- (5) N. R. Langley and J. D. Ferry, *Macromolecules*, **1**, 353 (1968).
- (6) N. R. Langley, *Macromolecules*, **1**, 348 (1968).
- (7) J. D. Ferry, "Viscoelastic Properties of Polymers," 2nd ed, Wiley, New York, N. Y., 1970, p 368.
- (8) S. F. Edwards and W. H. Stockmayer, *Proc. Roy. Soc., Ser. A*, **332**, 439 (1973).
- (9) We are indebted to Dr. Dennis J. Massa for this determination and to Professor H. Yu for use of the apparatus.
- (10) E. R. Fitzgerald, *Phys. Rev.*, **108**, 690 (1957).
- (11) D. J. Plazek, M. N. Vrancken, and J. W. Berge, *Trans. Soc. Rheol.*, **2**, 39 (1958).
- (12) K. Ninomiya, J. R. Richards, and J. D. Ferry, *J. Phys. Chem.*, **67**, 327 (1963).
- (13) M. L. Williams, R. F. Landel, and J. D. Ferry, *J. Amer. Chem. Soc.*, **77**, 3701 (1955).
- (14) Reference 7, p 316.
- (15) J. F. Sanders, Ph.D. Thesis, University of Wisconsin, 1968.
- (16) P. Thirion and R. Chasset, *Rev. Gen. Caout.*, **41**, 271 (1964).
- (17) We are indebted to Mr. F. H. M. Nestler for developing this program and Miss Hsin Huang for performing the calculations.
- (18) D. J. Plazek, *J. Polym. Sci., Part A-2*, **4**, 745 (1966).
- (19) Reference 7, Chapter 4, eq 9, 43, and 50.
- (20) E. R. Fitzgerald, L. D. Grandine, Jr., and J. D. Ferry, *J. Appl. Phys.*, **24**, 650 (1953).
- (21) J. D. Ferry, L. D. Grandine, Jr., and E. R. Fitzgerald, *J. Appl. Phys.*, **24**, 911 (1953).
- (22) J. F. Sanders and J. D. Ferry, *Macromolecules*, **2**, 440 (1969).
- (23) N. R. Langley and K. E. Polmanteer, *J. Polym. Sci.*, **12**, 1023 (1974).
- (24) R. E. Cohen and N. W. Tschoegl, *Int. J. Polym. Mater.*, **2**, 49 (1972).
- (25) O. Kramer, R. Greco, and J. D. Ferry, *Bull. Amer. Phys. Soc.*, **18**, 318 (1973).
- (26) O. Kramer, R. Greco, R. A. Neira, and J. D. Ferry, *J. Polym. Sci.*, in press.